Supporting Information

Valencia-Burton et al. 10.1073/pnas.0907495106

SI Text

Construction of the Plasmid pMB133 with Regulated RNA Synthesis. To create a plasmid with regulated RNA expression (pMB133), the first T7 promoter of vector pETDuet-1 (Novagen) was modified to contain *tet* operator sequences instead of *lacO* for independent induction of RNA. 2 x *tet*O_2 was amplified from pRS4D1 (1) and cloned downstream of the promoter TATA box by PCR-directed insertion as described before (2). A fragment corresponding to two copies of an RNA aptamer binding eukaryotic initiation factor 4A (eIF4A) was amplified from pMB23 (2) by PCR and cloned downstream of the modified promoter between HindIII-NotI sites. The *tetR* gene was amplified by PCR from pRS4D1 and cloned in the second multiple cloning site of the same plasmid between NdeI-XhoI sites. Expression of the *tetR* gene would proceed from the second unmodified T7 promoter. The resulting plasmid, pMB133, turns off the expression of the aptamer-containing RNA via TetR-*tetO* interactions in the promoter region. This inhibition is released in the presence of anhydrotetracycline which results in RNA expression. Cloning of this plasmid was done in *E. coli* strain XL10-Gold (Stratagene).

Testing Fluorescence Dynamics in *E. coli* Cells in Absence of New RNA Synthesis. *E. coli* BL21(DE3) cells were transformed with plasmids pMB33 and pMB133, which express the complete inducible RNA labeling system. Cells were grown at room temperature in LB medium supplied with antibiotics and IPTG to induce expression of labeling protein fragments and the repressor of RNA synthesis. Growth was continued for 2 days at room temperature to allow full repression of the system (no RNA-dependent fluorescence). At this point, the culture was split; half of the culture was treated with the RNA inducer ATc (250 ng/ml), whereas the other half was allowed to grow in parallel as control for ATc-independent fluorescence or derepression of the promoter. Cells were grown in the presence of ATc for 2.5–3 h at room temperature. Fluorescence of both induced and control cultures were measured by flow cytometry. The fluorescence of the uninduced culture (no ATc) was subtracted from that of the induced culture at every time point in this experiment. Cultures were next washed and diluted 2-fold in new LB media supplied with antibiotics and IPTG to remove ATc and to keep cells in exponential growth. Fluorescence of the cultures was measured by flow cytometry at indicated time points after the removal of ATc. Background fluorescence (from the control cultures with no ATc) was then subtracted from the values obtained by FACS. Fig. S2 shows the corrected fluorescence after removal of ATc relative to that of a fully induced culture (before removal of ATc).

Estimation of the Number of EGFP Molecules Per Cell. Intensity calibration measurements used the same microscope and filter combination; but instead of the flat illumination field, a nearly diffraction limited spot was used for illumination by filling the back aperture of the objective with a collimated light. Emitted light was projected through a pinhole onto an avalanche photodiode read using a custom LabView program (3). All measurements were taken at dark ambient conditions and at room temperature.

Measurements of RNA Concentration. Total cellular RNA was isolated from *E. coli* cell culture at certain time points after ATc induction. Target RNA concentration was measured using competitive PCR as described (2). *mre*B transcript was used as a standard.

Correlation Analyses of Circumferential Fluorescence Distribution in Single Cells. All image processing was carried out using ImageJ running on a Dell personal computer. The fluorescence distributions along the long axis at the two edges in individual cells were analyzed by drawing parallel lines and recording scan profiles; cells were treated as symmetric units (equal number of points for each side were collected). Each profile was recorded at least in duplicate, averaged, and used in correlation analyses (Fig. 4 and Fig. S10).

1. Blake WJ, Kaern M, Cantor CR, Collins JJ (2003) Noise in eukaryotic gene expression. *Nature* 422:633–637.
2. Valencia-Burton M, McCullough RM, Cantor CR, Broude NE (2007) RNA visualization in live bacterial cells using fluorescent protein complementation. *Nat Methods* 4:421–427.
3. Sabanayagam CR, Sabanayagam CR, Eid J, Meller A (2004) High-throughput scanning confocal microscope for single molecule analysis. *Appl Phys Lett* 84:1216–1218.

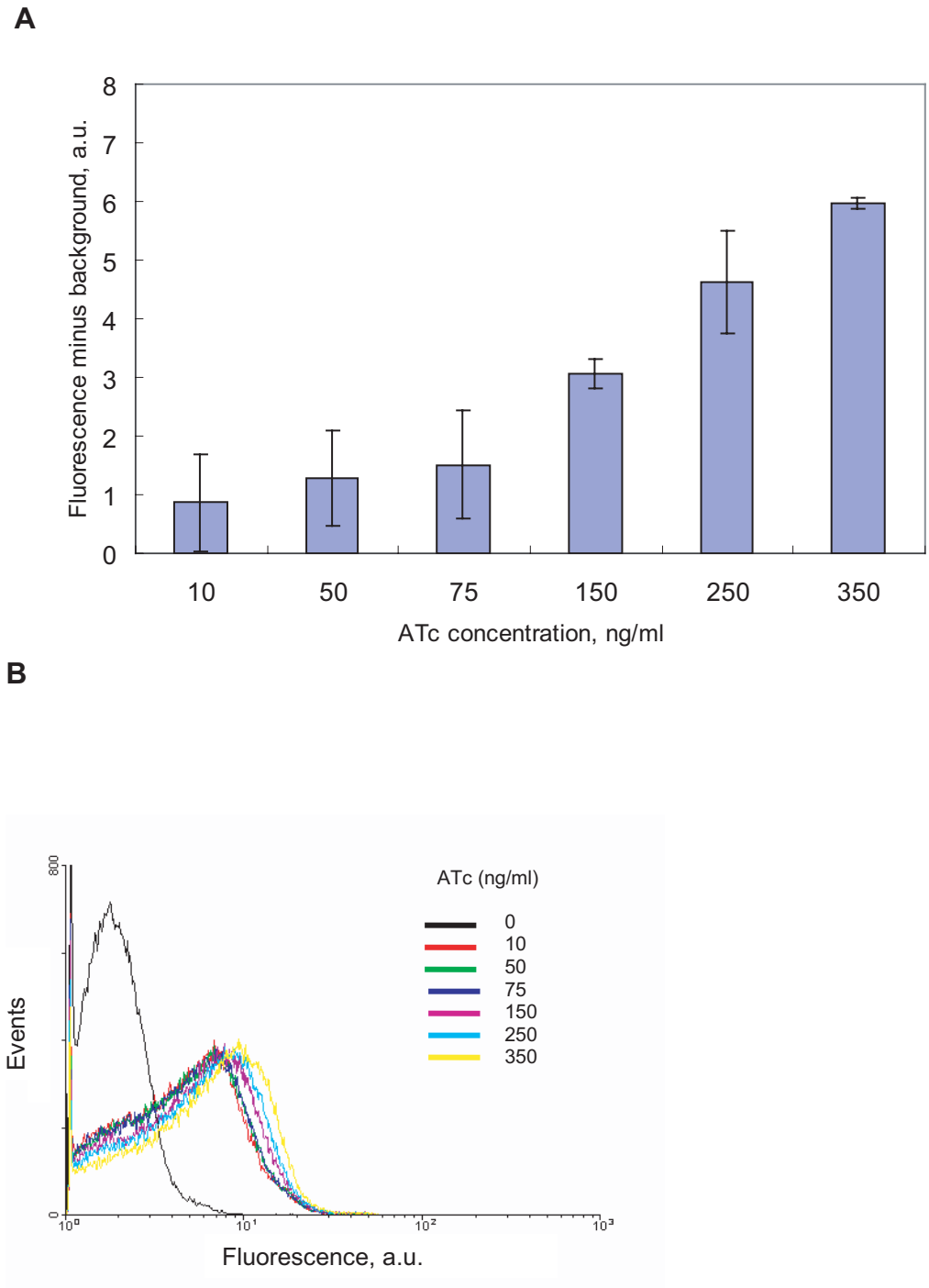

Fig. S1. Fluorescence of *E. coli* cells increases with increasing concentration of RNA inducer, ATc. (*A*) Average fluorescence obtained by flow cytometry in three independent experiments is shown. Background fluorescence (signal independent of ATc induction) was subtracted in every measurement. (*B*) Fluorescence distributions of cells at increasing concentrations of the RNA inducer ATc in one representative experiment.

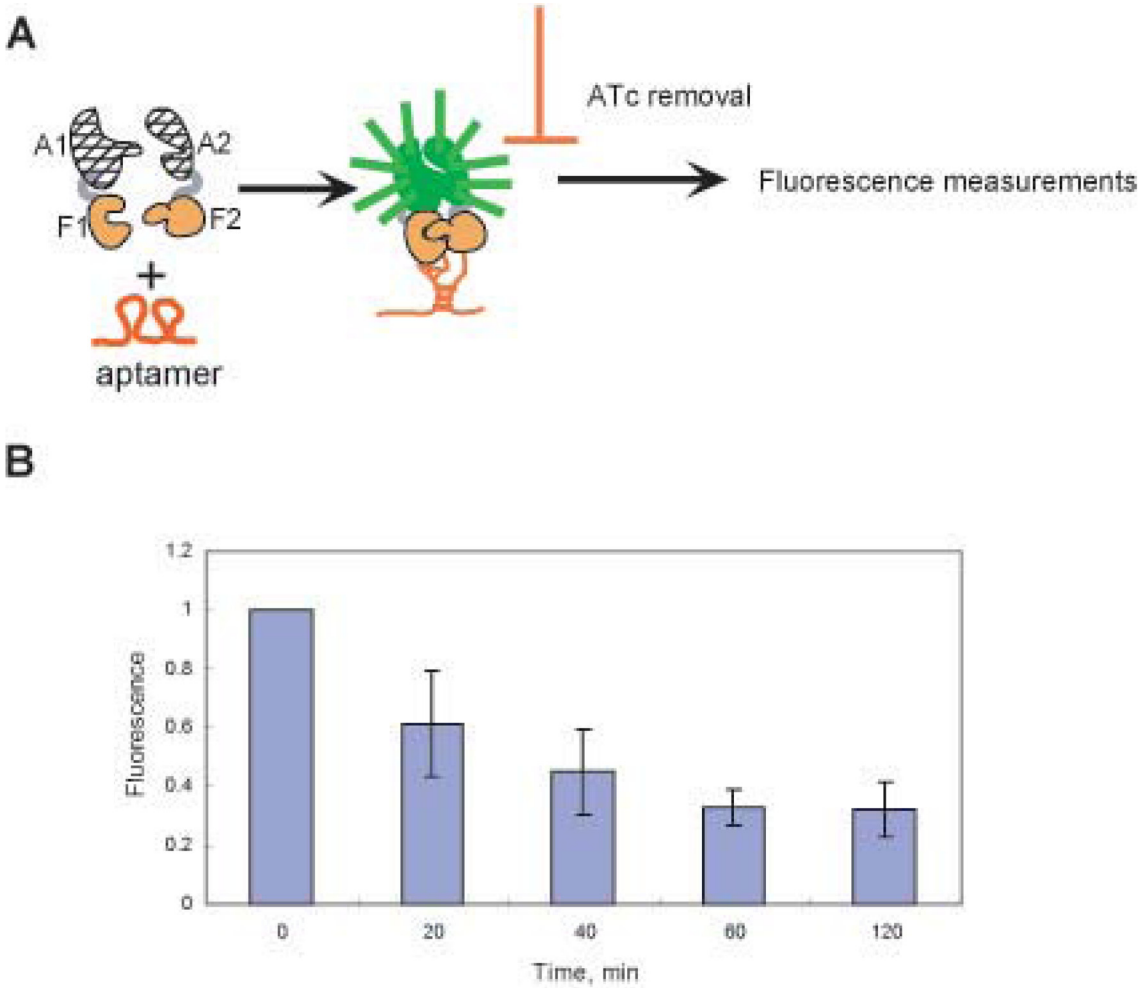

Fig. S2. Fluorescence decrease in *E. coli* cells in the absence of new RNA synthesis. (*A*) Experimental scheme. (*B*) Fluorescence changes in *E. coli* cells expressing RNA-dependent fluorescent complex after shutting down RNA synthesis. Bars represent fluorescence of cells after removal of ATc normalized to fluorescence of a fully induced culture. Average of four independent experiments is shown.

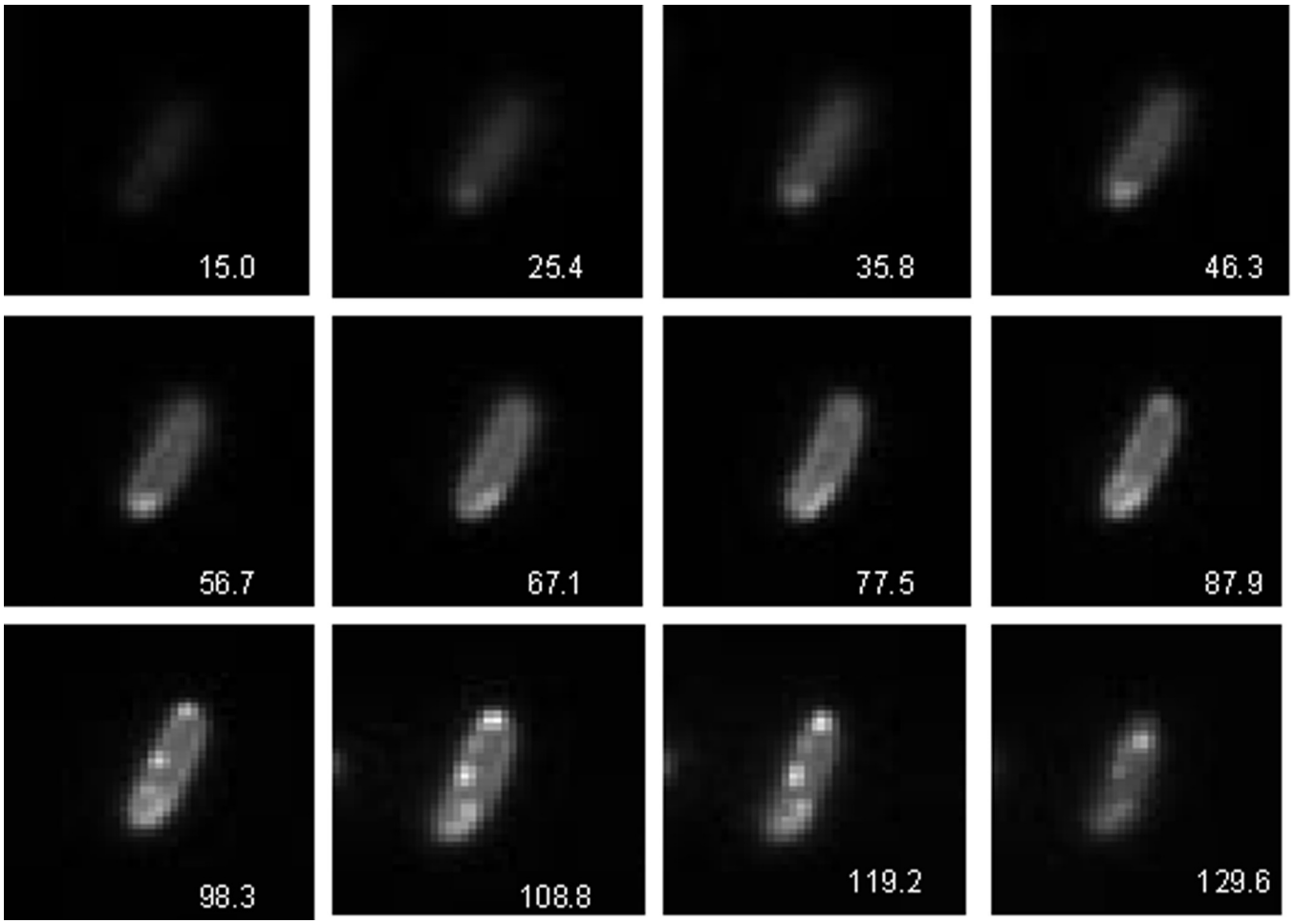

Fig. S3. Time-lapse images of a single cell expressing RNA (full set of images to accompany Fig. 3*A*).

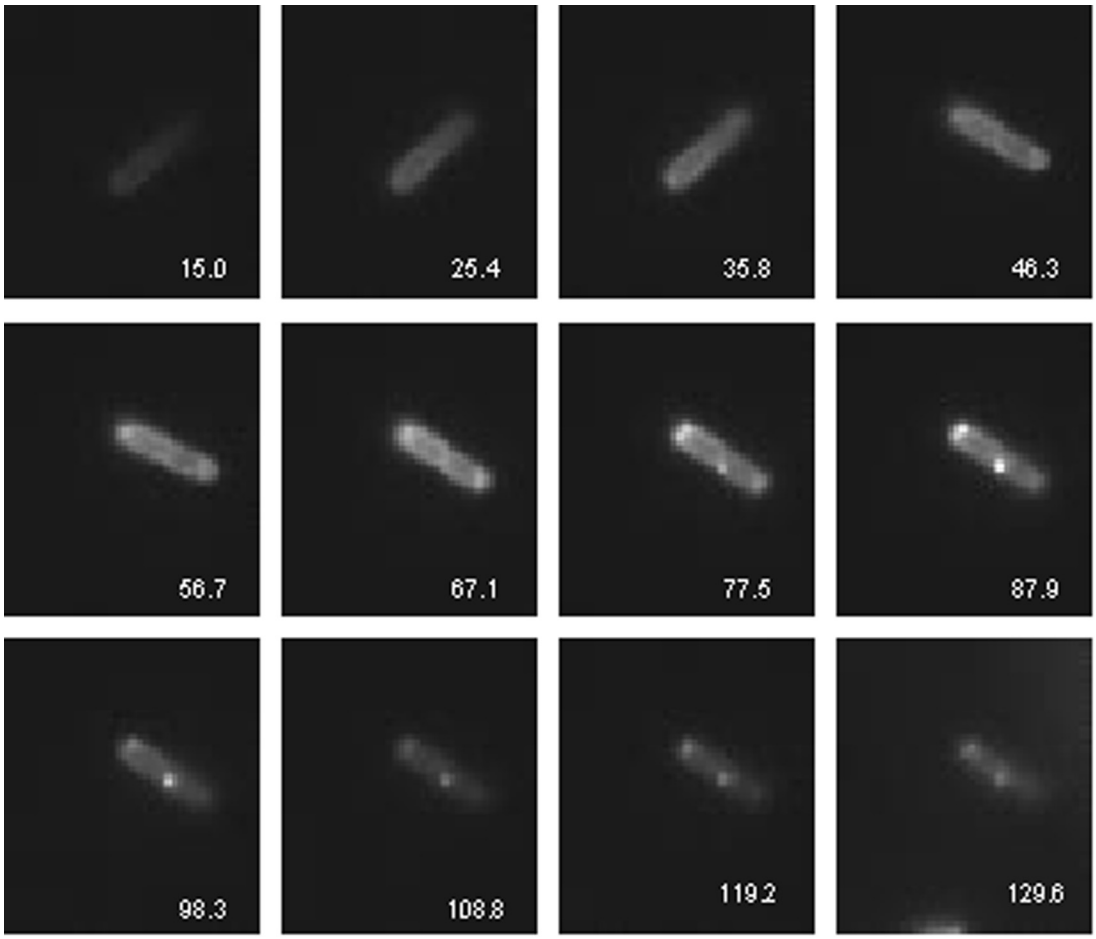

Fig. S4. Time-lapse images of a single cell expressing RNA (full set of images to accompany Fig. 3*B*).

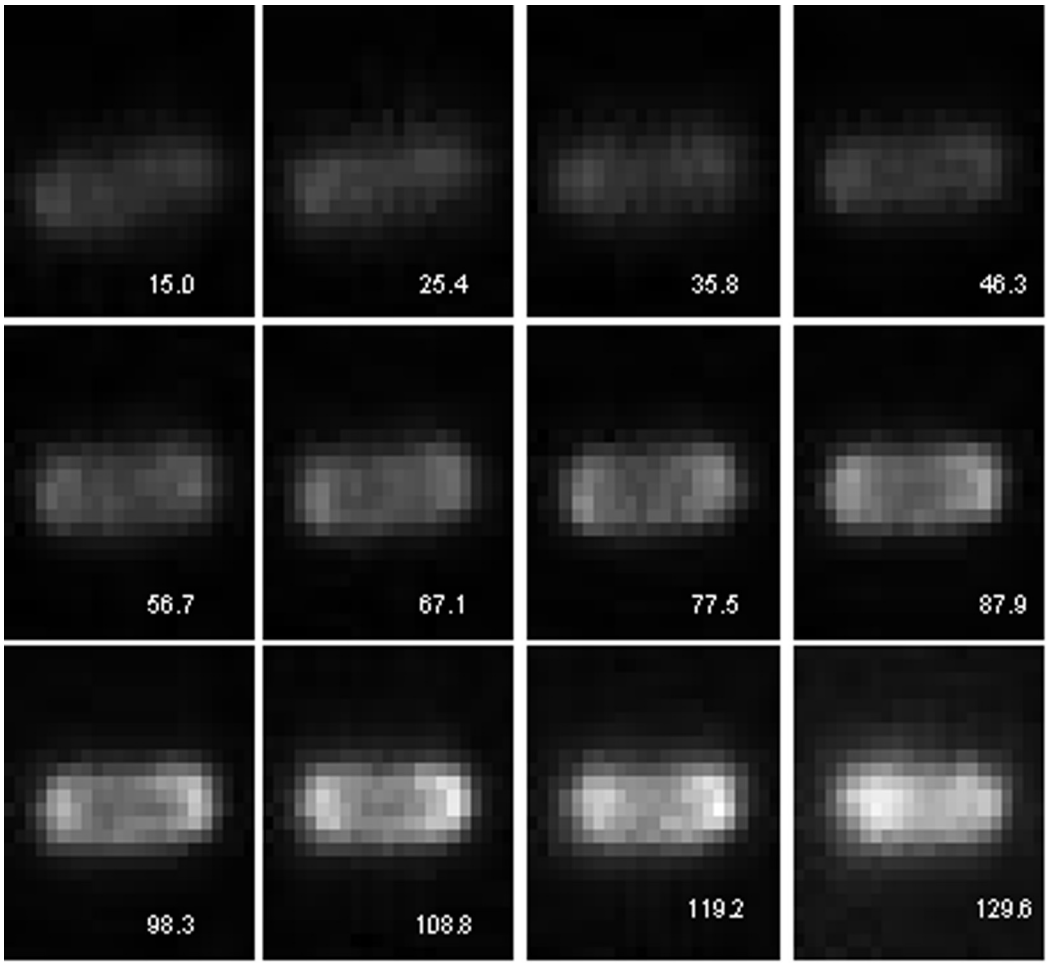

Fig. S5. Time-lapse images of a single cell expressing RNA (full set of images to accompany Fig. 3C).

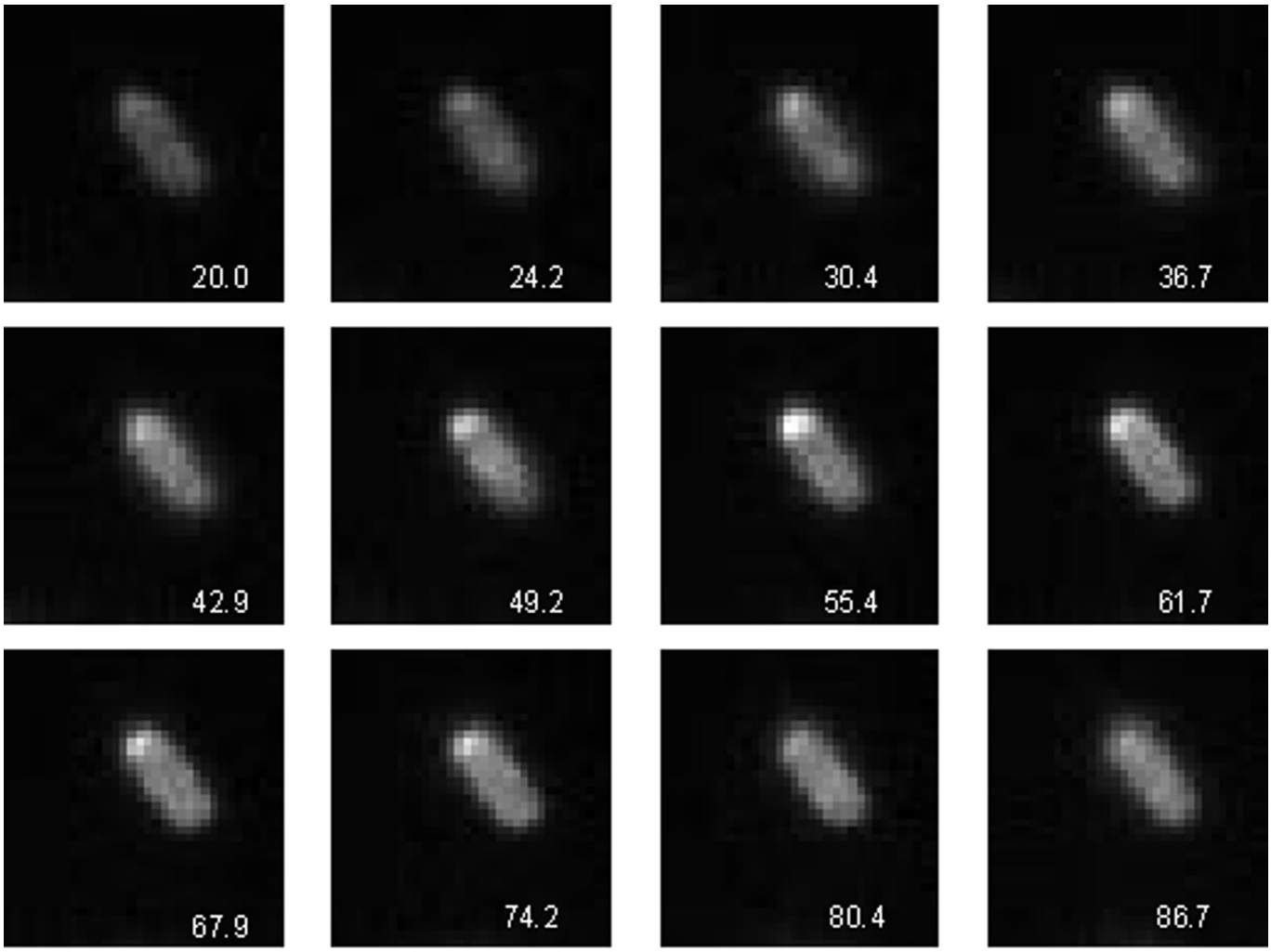

Fig. S6. Time-lapse images of a single cell expressing RNA (full set of images to accompany Fig. 3*D*).

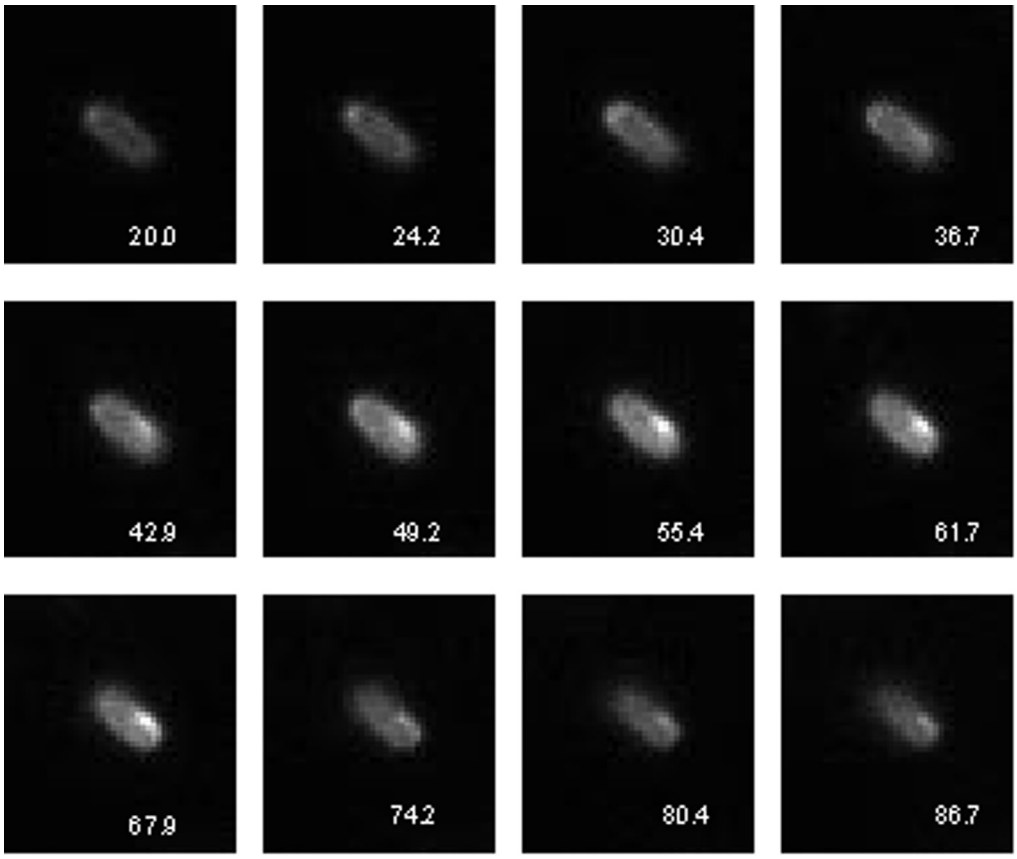

Fig. S7. Time-lapse images of a single cell expressing RNA (full set of images to accompany Fig. 3*E*).

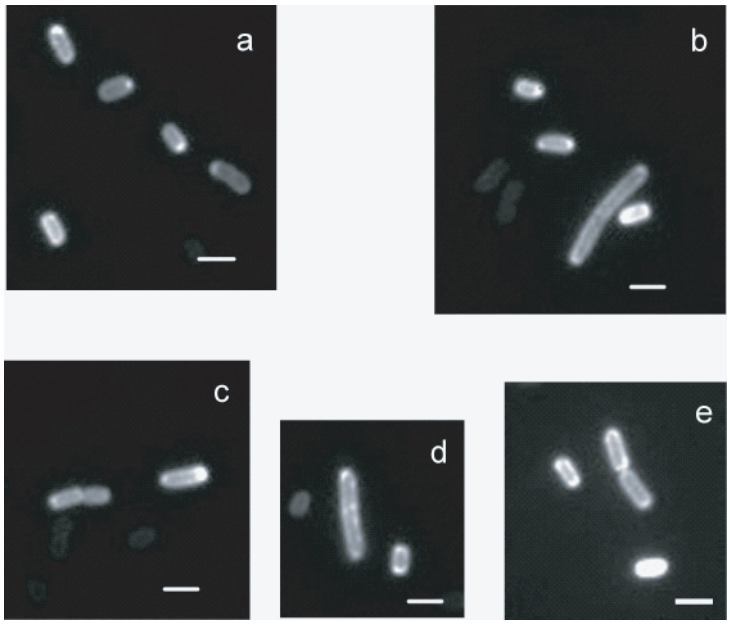

Fig. S8. Examples of *E. coli* cells expressing RNA with preferentially lateral fluorescence distributions. The middle of cells is dimmer than the edges. Scale bar, 2 μm.

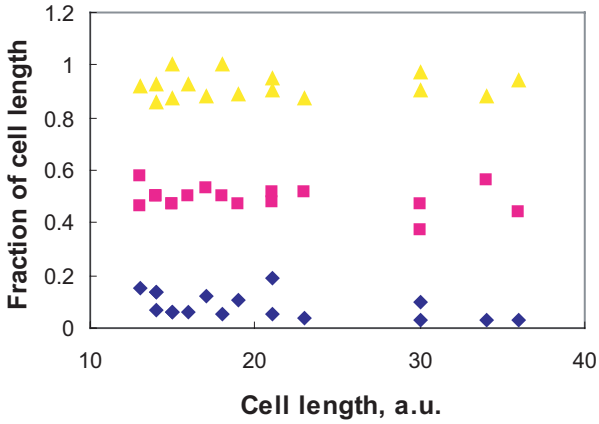

Fig. S9. Localization of RNA-linked fluorescence at the poles and at the mid-cell positions. The position of each focus was measured with respect to one end of the cell. Cell length, in arbitrary units, is plotted against position of foci (given as a fraction of cell length).

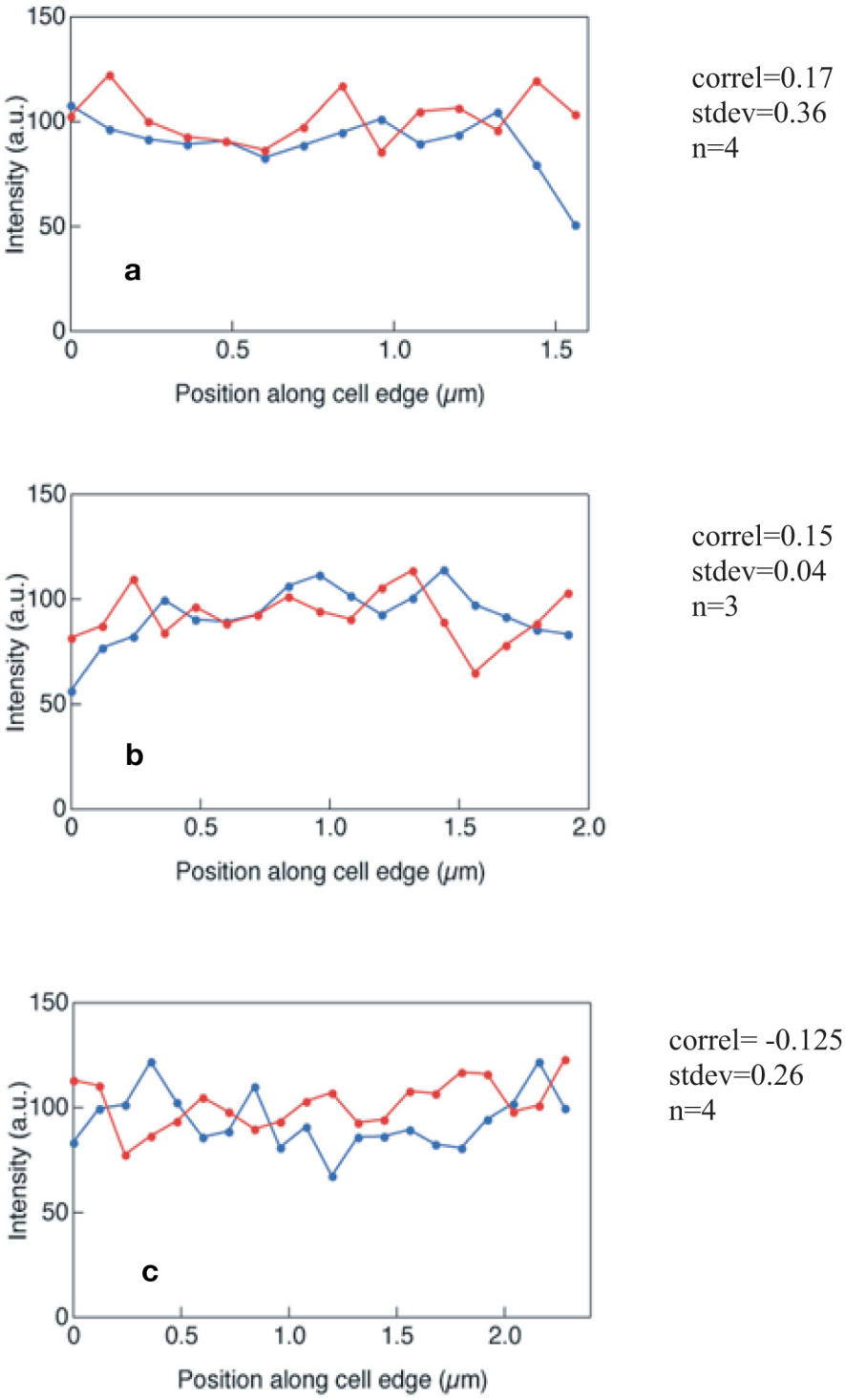

Fig. S10. Examples of RNA-expressing *E. coli* cells with fluorescence distribution at the two cell edges in counter phases (*n*, number of replicate measurements).

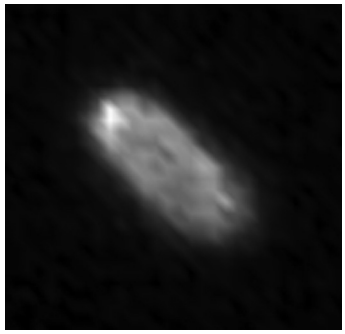

Movie S1. *E. coli* cell expressing RNA. Cells carrying two plasmids pMB133 and pMB33 were induced in culture with IPTG to express fusion proteins and TetR protein. Cells were then immobilized on a cover glass and induced with 250 ng/ml ATc for RNA synthesis. Images were taken with 2-min intervals. Movie contains 32 frames spanning 66.7 min. This *E. coli* cell displays dynamic behavior of fluorescent accumulation at the pole, which then disappears, and new accumulation is visible at other location.

Movie S1 (AVI)

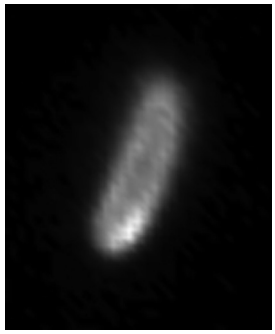

Movie S2. See legend to Movie S1. In this cell, accumulations of fluorescence at the mid-cell and quarter-cell positions are visible.

Movie S2 (AVI)

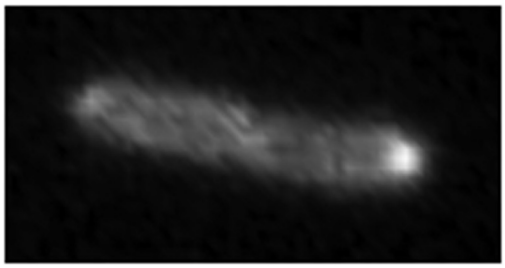

Movie S3. See legend to Movie S1. This *E. coli* cell is close to division. The dynamic RNA network is discernible in several frames.

Movie S3 (AVI)